

Stiffness and energy losses in cylindrically symmetric superconductor levitating systems

Carles Navau^{†‡} and Alvaro Sanchez^{†‡}

[†] Grup d'Electromagnetisme, Departament de Física,

Universitat Autònoma de Barcelona, 08192 Bellaterra, Barcelona, Catalonia, Spain and

[‡] Escola Universitària Salesiana de Sarrià, Rafael Batlle 7, 08017 Barcelona, Catalonia, Spain.

Stiffness and hysteretic energy losses are calculated for a magnetically levitating system composed of a type-II superconductor and a permanent magnet when a small vibration is produced in the system. We consider a cylindrically symmetric configuration with only vertical movements and calculate the current profiles under the assumption of the critical state model. The calculations, based on magnetic energy minimization, take into account the demagnetization fields inside the superconductor and the actual shape of the applied field. The dependence of stiffness and hysteretic energy losses upon the different important parameters of the system such as the superconductor aspect ratio, the relative size of the superconductor-permanent magnet, and the critical current of the superconductor are all systematically studied. Finally, in view of the results, we provide some trends on how a system such as the one studied here could be designed in order to optimize both the stiffness and the hysteretic losses.

I. INTRODUCTION

Superconducting levitation results from the interaction between an applied field and the currents in a superconductor[1]. Macroscopically, a type-II superconductor with strong pinning can be studied using the critical state model[2]. Within this framework, currents with constant density are induced in the superconductor due to a variation of the applied field it feels, either for a change in the value of a uniform field or for a displacement of the superconductor in a non-uniform field. A relative movement between a superconductor and a permanent magnet will thus result in a magnetic force between the induced currents in the superconductor and the field of the magnet. If this force compensates the weight of the levitated object and the conditions for stability hold, the object will stably and passively levitate[3].

Earnshaw proved that only diamagnetic materials can passively and stably levitate[4]. Although type-I superconductors can levitate (actually, they can produce large levitation forces because of their strong diamagnetism), the use of type-II superconductors has become more useful because of their rigidity. The rigidity arises from the pinning of the flux lines and allows a continuous range of passive equilibrium positions[5]. Yet, the use of the type-II superconductors results in an energetic loss due mainly to the magnetic hysteresis[6].

A superconducting bearing is a system composed, in its simplest form, of a superconductor and a permanent magnet. The rigidity and the losses are important factors in the design of a bearing. Actually, complicated types of bearings have been designed in order to improve rigidity and losses of the whole system. An excellent review on

superconducting bearings can be found in [7].

Measurements of stiffness[8, 9] and losses[10, 11] in levitating superconductor-permanent magnet bearings have been recently published. From the theoretical point of view, the study of stability and losses in high T_c -permanent magnet bearings is a complicated task, mainly due to the trouble of finding the current penetration inside the superconductor when the applied field is not homogeneous. Several models have been presented. In [12] and [13] we proposed approximate analytical expressions for stiffness and losses, assuming both a small superconductor and approximate demagnetizing factors. In Ref. [9] the stiffness of a bearing with a thin film superconductor was calculated, considering the exact form of the applied field and assuming a fully penetrated thin superconductor. Based on the interaction between dipole images, Kordyuk [14] calculated the force and energy losses on a permanent magnet over a flat ideally hard superconductor. Using the same model, Hull and Cansiz[8] calculated the stiffness of such a system.

In Refs. [15, 16] a model to calculate the current penetration of currents inside a finite cylinder, taking into account both the demagnetization factors and the radial components (and inhomogeneity) of the applied field, was presented. The model, based on the critical state and on the minimization of magnetic energy, was used for calculating the current penetration and levitation forces in the case of a cylindrically symmetric bearing system [16]. In this work, we will extend the application of the model to calculate, not only the current penetration and the levitation force, but the rigidity and the hysteretic energy losses resulting from the reaction of the system to an eventual vibration. We will study the dependence of these properties upon both intrinsic parameters of the superconductor (its critical current) and geometrical parameters (aspect ratio of the superconductor and relative size between superconductor and permanent magnet).

This paper is structured as follows. In Section II we review the calculation model used, focusing on its applica-

[‡]To whom correspondence should be addressed (alvar.sanchez@uab.es)

tion to the present case of vertical vibrations. In Section III we define the stiffness and the hysteretic losses and expound some general trends of these parameters. Results for the case of cylindrical symmetry are presented in Section IV. Section V is devoted to the discussion of the results and their use to optimize a real system. Finally, the conclusions can be found in Section VI.

II. MODELIZATION

We consider a zero-field cooled type-II cylindrical superconductor (SC) of radius R and length L located, initially, very far from a coaxial cylindrical permanent magnet with uniform magnetization in the direction of its axis (PM). The PM has radius a , length b , and magnetization M_{PM} . A scheme of the system is shown in Fig. 1. We shall use cylindrical coordinates with the origin located at the top face of the PM. We consider that the PM is fixed and that the SC, initially above it, can be moved towards or away from it. We define the distance between the PM and the SC, d , as the z -height of the bottom face of the SC. The general process of descending the SC from a very distant position to a minimum distance, d_{\min} , and then ascending it to far from the PM, $d \rightarrow \infty$, is called the major loop.

We want to simulate the response of the SC after a small vibration of the system, produced at some point of the major loop. A vibration is regarded as a change in the actual direction of the movement and the subsequent return to the original position. This movement is referred to as a minor loop (see Fig. 1). In this work, we only consider cylindrically symmetric situations. That is, we only consider movements of the SC along the axial direction, during both major and minor loops.

The response of a finite cylindrical SC in the critical state and after a movement in the presence of a non-uniform (but cylindrically symmetric) applied field has been studied in [16] using a numerical procedure described in [15]. The model includes the following assumptions, besides the cylindrical symmetry: a) no equilibrium magnetization for the SC is considered; b) the PM is not affected by the presence of the SC; and c) the superconductor is assumed to be in the critical state. (The force creep due to thermal demagnetization has been recently studied by Qin et al [17]). We calculated in [16] the levitation force during a major loop and studied the principal characteristics of that force and its dependence on important parameters of the system. We now briefly review the main steps in the calculation of the desired magnitudes. After a variation of the position of the superconductor, we calculate the currents induced in the superconductor by imposing that these currents tend to minimize the magnetic energy of the superconductor. When a variation of the direction of movement is produced, currents in reverse direction begin to enter the superconductor. In this latter case, we calculate the response of the SC using the typical procedure of the

critical state [18] keeping the already set currents and calculating the penetration of new reverse ones in the same way as for the initial stage but considering the variation of the field.

For a given current distribution inside the superconductor, the magnetic force between the currents and the external applied field in the case of cylindrical symmetry has only a z -component given by

$$F_z = 2\pi\mu_0 \int_V J_c(\rho, z) H_\rho^a(\rho, z) \rho \, d\rho, \quad (1)$$

where $V = \pi R^2 L$ is the volume of the SC and H_ρ^a is the radial component of the applied field created by the PM.

Although in the described procedure we could implement a dependence of the critical current with the internal field, in this work we use a constant critical current J_c , for the sake of simplicity. In that case, Eq. 1 becomes

$$F_z = 2\pi\mu_0 J_c \int_\Omega H_r^a(\rho, z) \rho \, d\rho, \quad (2)$$

being Ω the current penetrated region. Ω depends not only on the value of J_c but on the geometry of the sample, because of the demagnetizing fields. If the superconductor becomes fully penetrated by currents, $\Omega = V$ and the vertical force is proportional to J_c .

Unless the contrary is explicitly written, we will consider the following parameters: $a = b = R = L = 0.01\text{m}$, $J_c = 2.81 \cdot 10^7 \text{A/m}^2$, and $M_{PM} = 7.95 \cdot 10^5 \text{A/m}$. The geometrical values have been chosen among the typical ones in levitation experiments. The value for M_{PM} is such that $\mu_0 M_{PM} = 1 \text{T}$. J_c is chosen to equal H_0/R , being H_0 the magnetic field at the origin of coordinates (the center of the top face of the PM). Using these parameters, the field H_0 can be considered as a typical field of penetration of the superconductor since when the superconductor is at zero distance (so the applied field in the center of its lower face is H_0) the superconductor is considerably penetrated by currents (although not completely penetrated because the sample is finite and $H_p = J_c R$ is the penetration field for an infinite sample in a uniform applied field). We will see below why this is an appropriate parameter. The use of non-normalized variables allows the easier comparison with experimental values. However, an adequate normalization could reduce the number of parameters of the system (see Ref. [12]). In this work, we will use non-normalized variables for the calculations but will discuss the results in relation to important dimensionless parameters.

In Fig. 2 we show calculated results illustrating the general shape of the major loop of the force-distance curve together with some minor loops at several starting distances. In the inset, a detail of one minor loop is also showed. Since the penetration of currents in the critical state is a hysteretic phenomenon, so the force is, in both the major and the minor loops. In Fig. 3 we show calculated current penetration profiles corresponding to several points of one minor loop (we have chosen

the loop in the inset of Fig. 1; the plotted points are marked there). We observe the hysteretic process of current penetration causing the hysteresis in the force during a minor loop. As we shall see in detail in the next sections one can analyze the stability and the hysteretic losses of the system from the shape of these minor loops.

III. DEFINITIONS AND GENERAL CONSIDERATIONS

A. Restoring force and stiffness

A useful mechanical system, including those with levitating components, is often required to be stable in all directions. Any variation of the position of the working point of a rigid solid must result in a restoring force that tend to return the system to its original place. Considering small displacements from the working position, one could define the stiffness as the first order spring constant of the restoring force. Thus, we define a stiffness matrix whose elements are

$$\kappa_{\alpha\beta} = -[\nabla_{\beta} F_{\alpha}]_{\mathbf{r}_0}. \quad (3)$$

The physical meaning of the $\alpha\beta$ -element is the following: it is the first order spring constant of the restoring α -component of the force, after a variation of the working point \mathbf{r}_0 in the β -direction. The minus sign is set by convenience, as discussed below.

In this work we consider a cylindrical system in which the working position and the vibrations of the system will always maintain the cylindrical symmetry. The force after one of such variations will have only axial component, which results in $\kappa_{\rho z} = \kappa_{\theta z} = 0$. In that case, thus, only the component κ_{zz} should be accounted for. From Eq. 3, we have that

$$\kappa_{zz}(z_1) = - \left[\frac{\partial F_z^{ml}}{\partial z} \right]_{z \rightarrow z_1}. \quad (4)$$

The upper index ml indicates that the force that should be considered is the one within the minor loop. This is because, in the case of type-II superconductors, the force is hysteretic, so the force after the start of a vibration is the one inside a minor loop.

Although in this work we only calculate the κ_{zz} component, it is interesting to discuss some general properties of the stiffness matrix in the case of a cylindrically symmetric working point. Since there is no angular dependence, any displacement of the superconductor in the angular direction should not modify the current distribution so the restoring force is zero. Thus, $\kappa_{\rho\theta} = \kappa_{\theta\theta} = \kappa_{z\theta} = 0$. Moreover, by symmetry, any displacement in the radial direction will tend to give a restoring force with no-angular component, resulting in $\kappa_{\theta\rho} = 0$. In that latter case there will appear both a restoring force in the radial direction (and stiffness $\kappa_{\rho\rho}$) which is the lateral restoring force,

and also a vertical force (with stiffness $\kappa_{z\rho}$) which will tend to modify the height of the working point.

The stiffness coefficients can have different values for the same working point depending on how that working point has been achieved. This is due to the hysteresis in the behavior of the levitation force in type-II superconductors. Although the stiffness is only calculated from the force during a minor loop, that force depends on the previous magnetic history of the superconductor. In the case considered here of vertical movements, we expect to obtain different value for the $\kappa_{zz}(z_1)$ for a given z_1 when considering a minor loop produced at a height z_1 during the general descending stage or when considering a minor loop produced in the same z_1 but in the major ascending stage.

Finally, the minus sign in Eq. 3 is set for convenience, since in this case the condition for vertical stability is $\kappa_{zz} > 0$. If, at some equilibrium position, an increment in the vertical distance is produced ($\partial z > 0$), the levitation force should decrease ($\partial F_z < 0$; the weight of the object would tend to return it to the equilibrium distance). On the other hand, if the levitated object is pushed down ($\partial z < 0$), the levitation force should increase ($\partial F_z > 0$). In both cases $\kappa_{zz} > 0$.

B. Hysteresis and energy losses

The hysteretic energy losses can be defined as the work done by the system during a complete minor loop. They can alternatively be defined as the energy needed to force a levitating object to follow a minor loop and return to the original position. The only difference is the sign of the two expressions. To avoid this ambiguity, we define the hysteretic energy losses as

$$E = \left| \oint_{ml} \mathbf{F} d\mathbf{r} \right|, \quad (5)$$

where the subindex ml indicates that the integration should be done over the minor loop.

This general expression can be simplified when considering that the cylindrical symmetry is preserved through the minor loop. In that case, $F_{\rho} = F_{\theta} = 0$. If we consider that the minor loop runs between z_1 and z_2 (with $z_1 < z_2$) and name E_{zz} the resulting hysteretic energy losses, Eq. 5 is simplified into

$$E_{zz}(z_1) = \int_{z_1}^{z_2} |F_z^{\uparrow} - F_z^{\downarrow}| dz, \quad (6)$$

where F_z^{\uparrow} and F_z^{\downarrow} refer, respectively, to the force during the ascending and descending movements of the superconductor during the considered minor loop.

The point z_1 at which E_{zz} is calculated is the starting point of the vibration only if produced during the major descending stage. If the minor loop is produced during the major ascending stage, then z_1 is the reversing point of the vibration. The reason is that, differently from

the stiffness coefficient κ_{zz} , the energy losses at a given point do not depend (in the critical state framework) on the previous magnetic history of the superconductor. In the case considered here of vertical movements, $E_{zz}(z_1)$ does not depend on whether z_1 is the one in the general descending stage or in the ascending one. This fact can be understood from Eq. 5. Since in the calculation of E_{zz} one must consider the difference between forces during the minor loop, the eventual contribution of the frozen currents to the force is eliminated from the equation, resulting in the non-hysteretic behavior of E_{zz} .

IV. RESULTS FOR κ_{zz} AND E_{zz} .

In this section we present calculations of the vertical stability and the hysteretic energy losses of a cylindrically levitated system. We systematically study the dependence of stiffness κ_{zz} and losses E_{zz} on different relevant parameters of the system such as the critical current of the SC, the aspect ratio of the SC, and the relative dimensions of the SC and the PM. We consider in all cases minor loops started at a fixed distance ($z_1 = 0.005\text{m}$) and amplitude of the vibration ($\Delta z = 0.0025\text{m}$).

Both coefficients κ_{zz} and E_{zz} have some general features independently of the parameters of the system (except in some extreme limits). During the initial descending, both κ_{zz} and E_{zz} increase as z_1 decreases owing to the increasing of the field gradient and the larger penetration[19]. As stated above, κ_{zz} is hysteretic whereas E_{zz} is not. Another general feature is that, in the returning stage, the stiffness becomes negative for a large enough z_1 's. This fact, already pointed out in [12], is produced because for large enough z_1 's the variation of the applied field is small and the currents hardly enter inside the sample. The minor loops have then to follow the major one, resulting in a negative stiffness (positive initial slope). Actually, depending of the shape of the PM, it may also exist a non stable region in the major descending loop[12].

A. J_c dependence

In Fig. 4 we show the calculated κ_{zz} (Fig. 4-a) and E_{zz} (Fig. 4-b) as a function of the critical current J_c , for three values of the aspect ratio L/R of the SC, corresponding respectively to a thin film sample ($L/R = 1/5$), a regular size sample ($L/R = 1$), and a large sample ($L/R = 5$). In these calculations we have fixed the PM and the value of R (maintaining so the value a/R). We observe that the stiffness increases with increasing J_c , whereas E_{zz} has a maximum and tends to zero in both limits for low- J_c and high- J_c .

Results for the stiffness can be understood from a simplified model that considers a small PM and a very thin superconductor[9, 20]. Within this model, κ_{zz} has two

contributions:

$$\kappa_{zz}(z_1) = -\mu_0\pi R^2 L \left[-\chi_0 \left(\frac{\partial H_z}{\partial z} \right)^2 + M_z(z_1) \frac{\partial^2 H_z}{\partial z^2} \right]. \quad (7)$$

The first term in the Eq. 7 is independent of J_c and is related to the initial susceptibility of the SC, $\chi_0 = \frac{8R}{3\pi L}$ [18]. The second one depends upon the magnetization of the SC and, thus, upon J_c . Riise et al [9] reported that for a typical experimental setup the second term is much less important than the first one, so, for their very thin film, the stiffness was independent of J_c .

In the present general case, there are also two terms determining the stiffness. Consider a minor loop produced during the descending of the superconductor. The force, just at the starting point of the minor loop, z_1 , is

$$F_z^{fr}(z_1) = -2\pi\mu_0 |J_c| \int_0^L \int_{b(z',z_1)}^R H_\rho^a(\rho, z') \rho d\rho dz', \quad (8)$$

where $b(z', z_1)$ describes the current penetration profile. If at this point a minor loop starts, these already induced current are kept frozen (the superscript *fr* in Eq. 8 indicates this) and new reversal currents begin to enter. Then, the force can be calculated as

$$F_z(d) = F_z^{fr}(z_1) + F_z^{new}(d), \quad (9)$$

where F_z^{new} is the force due to the new induced currents:

$$F_z^{new}(d) = +2\pi\mu_0 |J_c| 2 \int_0^L \int_{a(z',d)}^R H_\rho^a(\rho, z') \rho d\rho dz', \quad (10)$$

being $a(z', d)$ the current profile of the new induced currents.

The coefficient κ_{zz} is calculated from Eq. 9 as

$$\kappa_{zz}(z_1) = - \left[\frac{dF_z^{fr}}{dd} + \frac{dF_z^{new}}{dd} \right]_{d \rightarrow z_1}. \quad (11)$$

Although the currents induced prior to the minor loop are kept frozen, the first term in Eq. 11 is different from zero because the applied field involved in the integral changes when varying z . This term corresponds to the $M_z(z_1) \frac{\partial^2 H_z}{\partial z^2}$ term in Eq. 7. It depends on J_c . On the other hand, the second term in Eq. 11 depends on the initial slope of the magnetization of the superconducting sample. It is the equivalent to the non-hysteretic term in Eq. 7. Within the critical state model, this term does not depend on J_c .

Considering a minor loop started at a given working point, increasing J_c increases the magnetization of the SC sample. The first term in Eq. 11 increases whereas the second one does not. The result is an increase of the stiffness, as can be seen in Fig. 4-a.

In the large J_c limit the force is almost non-hysteretic. Therefore, in this limit, the minor loop runs over the

major one and the stiffness can be approximately calculated directly from the slope of the major loop at a given distance.

The results for E_{zz} can be understood by looking at Fig. 5, where we have plotted several minor loops corresponding to the cases $L/R = 0.2$ (left), $L/R = 1$ (middle), and $L/R = 5$ (right), for different J_c values. (All the discussion below holds for the three figures, although the complete discussion is best seen in Fig. 5-a). For the case that J_c is small (actually, when it is small enough to produce a full penetration of the sample for a small variation in d) as soon as the minor loop is started, the sample is fully penetrated and as soon as the minor loop is reversed, the sample is again fully penetrated by currents circulating in the opposite direction. The result is an almost symmetric (with respect to the zero-force) behavior of the force during the minor loop. In that case, the levitation force is roughly proportional to the critical current (Eq. 2) and, from Eq. 6, we can see that the energy losses are

$$E_{zz} \simeq 4\pi\mu_0 |J_c| \int_{z_2}^{z_1} |g(h)| dh, \quad (12)$$

where $g(h)$ is defined as

$$g(h) = \int_0^R \int_h^{h+L} H_\rho^a(\rho, z) \rho d\rho dz. \quad (13)$$

For low J_c , thus, E_{zz} tends to zero, proportionally to J_c . As J_c increases, the full penetration is obtained only after a significant portion of the minor loop has been gone through. The minor loop becomes less and less symmetric, but at the same time, the value of the force increases. The resulting area of the minor loop increases for a range of not very large J_c 's. When J_c goes on increasing, no full penetration of reverse currents is achieved. Actually, for large J_c 's, the superconductor is hardly penetrated, either for direct currents or for reverse ones, so the losses are being reduced even though the value of the force increases. The resulting E_{zz} is thus tending to zero for large J_c .

In Fig. 4-b we observe that the maximum in the E_{zz} coefficient is displaced to lower J_c when the SC is larger. This is understood again in terms of the penetration. For longer superconductors (Fig. 5-b,c), the demagnetization fields are lower and, as a consequence, the running distance necessary to fully penetrate the SC is larger. The described crossover behavior of producing less hysteresis because of less penetration is attained, thus, at lower J_c 's. A more detailed description of the dependence on L/R will be given in Section IV A.

B. L/R dependence

In Fig. 6 we plot the dependence of κ_{zz} (Fig. 6-a) and E_{zz} (Fig. 6-b) on L/R for different values of the critical current. In order to study the dependence only on L/R

we have fixed the PM, the value of the R (maintaining so the relation a/R), and also the starting point ($z_1 = 0.005\text{m}$) and the amplitude ($\Delta z = 0.0025\text{m}$) of the minor loops.

We observe in Fig. 6-a that the stiffness significantly depends on L/R for low- J_c but hardly for high- J_c . The coefficient E_{zz} has a singular behavior. As seen in Fig. 6-b, for low critical current, E_{zz} increases for low L/R , and saturates for long L/R . On the other hand, for high J_c , it decreases all the time (within the L/R range shown), even for small L/R , saturating for long samples.

The argument exposed in the previous section explains also the behavior of κ_{zz} in the following way. The term in the stiffness depending on the magnetization is more important for high- J_c and, in this case, the magnetization slightly depends on L/R since almost no current penetrates the SC specially far from the PM. So, increasing L does not produces significant changes (except when the SC is very thin). On the other hand, when J_c is low, the sample is significantly penetrated by currents and the relation L/R plays an important role.

The behavior of E_{zz} can be more clearly understood by looking at Fig. 7-a and Fig. 7-b, where we have plotted the minor loops for different lengths and for a case of low critical current (Fig. 7-a) and a case of higher critical current (Fig. 7-b). When the current is low the force during a minor loop is almost symmetric with respect to zero-force value (Section IV A). Even in this low-current limit, when the superconductor is long, there are regions free of current, so the behavior departs from the symmetrical one. The departure, however, is not very strong since the applied field in the regions where no fully penetration is achieved is weak. In Fig. 7-a we observe this behavior and see that E_{zz} tends to increase as L/R decreases. The appearance of a maximum in the E_{zz} versus L/R curve for this case has the same origin as discussed in the previous section (a similar behavior of that shown in Fig. 5 could be observed in this case, but as function of L/R ; the difference is that now, when L/R is large, the minor loops tend to saturate to a constant shape instead of changing indefinitely). When the critical current is high, only when L/R is small the penetration is complete because the demagnetization effects are important in that case. When increasing L/R , the minor loops get less and less hysteretic until their shape (and thus, their area) is saturated (see Fig. 7-b). Actually, even in the case of high- J_c for thin enough samples the area of the minor loop should tend to zero, producing also a maximum in the force. In the scale used in Fig. 7-b, this is not seen.

Since both κ_{zz} and E_{zz} saturate for long superconductors, their value per unit volume decrease as $1/L$ for long enough superconductors.

C. a/R dependence

We study in this section the dependence of κ_{zz} and E_{zz} upon the ratio between the radii of the PM and the SC, a/R . We have maintained the value of R in order to not change the relation L/R . The value of b is also maintained and so is M_{PM} . We note, however, that when changing a , the applied field will change. In Fig. 8-a and Fig. 8-b we show, respectively, the calculated κ_{zz} and E_{zz} for three cases of J_c corresponding to 0.1, 1, and 10 times the relation H_0/R .

In Fig. 8-a we observe that there is a region of maximum stability (maximum value of stiffness) when the superconductor and the permanent magnet have similar radius (in Ref. [16] it was shown that also the magnitude of the force is larger when $a \simeq R$). E_{zz} shows a maximum at $a \simeq R$ and tends to zero for both $a \ll R$ and $a \gg R$ limits.

The results can be explained as follows. Given a magnetization M_{PM} of the permanent magnet, when the magnet has a radius $a \rightarrow 0$ the value of the applied field tends to zero and also does the levitation force. Both stiffness and energy losses should be zero in that limit. On the other hand, when the PM is much larger than the SC, in the region occupied by the superconductor the field is approximately homogeneous, resulting also in an almost null levitation force and, as a consequence, a very low stiffness and losses. In the intermediate regions, there should be, at least, one maximum. The fact that the maximum corresponds to $a \simeq R$ is related to the fact that, at a given distance from the PM, the applied field is most inhomogeneous at radial distances in the range of a . Therefore, SC's of radius $R \simeq a$ will feel larger variations in the applied field, resulting in a larger penetration of currents, which means a larger rigidity and, at the same time, larger losses, because of the larger hysteresis.

V. DISCUSSION

The levitation force of type-II superconductors is the result of the interaction between a distribution of induced critical currents and the external applied field. Stiffness and losses can be interpreted in terms of the current penetration profiles. In a qualitative way, the key parameter that accounts for the behavior of a bearing system is the relation between the field of penetration of the SC and the applied field of the PM. Other parameters are related with this. The penetration field for the superconductor depends on the critical current as well as on its dimensions and aspect ratio. (In this work we have only worked with cylinders, but in general, the penetration field also depends on the geometry of the superconducting sample). Actually, the larger the critical current is, the larger the penetration field is (proportionally) and the smaller L/R is, the larger that penetration field is (not in a proportional way [21]). The applied field felt by the superconductor depends on the magnetization of

the PM (proportionally, if considered uniform and constant), on the dimensions of the PM and on the distance between them.

The relation between these two fields determines the current penetration profiles in the following way: if the applied field felt by the SC is much smaller than its penetration field, current will hardly penetrate the SC, which will yield in almost non-hysteretic behavior and large forces. This condition can be achieved by several reasons (or by a combination of them), namely, high J_c , large L/R , low M_{PM} , small a (in relation to R), and/or small b . On the other hand, if the applied field felt by the SC is much larger than its penetration field, currents will penetrate a considerable amount of SC material after a small field variation (after a small movement of the SC). This will result in a highly hysteretic behavior. This condition will be fulfilled for low J_c , small L/R , high M_{PM} , and/or $a \simeq R$.

For the quantitative description of the stiffness and losses one should also take into account the actual value of the force. For example, even when there is large hysteresis, the area of a minor loop can be small if the applied field (and the force) is small (Fig. 5-a). Also, large hysteresis (almost symmetrical minor loops) does not necessarily mean a large stiffness. We have seen that large J_c 's increases the initial slope of a minor loop (in absolute value) although the hysteresis is reduced (Fig. 5 and Fig. 7).

VI. CONCLUSIONS

Using a model based on the critical-state approximation, we have been able to calculate the response of a levitating type-II superconductor in the presence of the non-uniform applied field created by a permanent magnet. We have focused our analysis on vertical vibrations that can occur at a given working point.

We have seen that when the radius of the PM and SC are similar, the stability of the system is maximized, although the losses are also the largest. As to the length of the superconductor, a very long sample can have a significant amount of material that contribute neither to the force, nor to the stiffness, nor to the hysteretic energy losses, resulting therefore in a useless waste of SC material. By increasing the critical current of the superconductor, the stability of the system is increased, whereas the losses could be reduced, if this critical current is high enough.

Optimization of a cylindrical bearing system should take into account all these results. Depending on the needs and the restrictions for a particular design, one should choose a permanent magnet and a superconductor that fit the needs. In particular, very high critical current could produce large stability with low losses. However if a thin film SC is used, even with such high critical current the sample could be easily fully penetrated and the losses would be important. If large levitation forces are needed,

a long superconductor with high critical current would be the optimum solution for the reduction of losses, without considerably reducing the stability.

In its current form, the present model is unable to describe some important phenomena of levitation, such lateral displacements (and lateral stiffness and hysteretic losses), movements at high frequencies (such that the critical state does not have time to be established inside the SC), force creep, or even finite geometries other than cylindrical. However, the same methodology could be eventually applied to these cases. If by some means, a procedure to obtain the current profiles inside the superconductor is found, the procedure described would be

valid for a phenomenological description of the levitation force. In particular, the relation between a typical penetration field of the superconductor and a typical applied field is expected to be the key parameter to explain the experimental data, even in situations different from the cylindrical symmetry described here.

Acknowledgements

We thank MCyT project BFM2000-0001 and CIRIT project 1999SGR00340 for financial support.

-
- [1] Brandt E H 1989 *Science* **243** 349
 - [2] Bean C P 1964 *Rev. Mod. Phys.* **36**, 31 (1964); Bean C P 1962 *Phys. Rev. L* **8** 250.
 - [3] Moon F C 1994 *Superconducting levitation* (New York: Wiley)
 - [4] Earnshaw S 1842 *Trans. Cambridge Philos. Soc.* **7** 97
 - [5] Brandt E H 1990 *Am. J. Phys.* **58** 43
 - [6] Coombs T A, Cansiz A and Campbell A M 2002 *Supercond. Sci. Tech.* **15** 831
 - [7] Hull J R 2000 *Supercond. Sci. Tech.* **13** R1
 - [8] Hull J R and Cansiz A 1999 *J. Appl. Phys.* **86** 6396
 - [9] Riise A B, Johansen T H, Bratsberg H, Koblishka M R and Shen Y Q 1999 *Phys. Rev. B* **60** 9855
 - [10] Terentiev A N, Lee H J, Kim C-J and Hong G W 1997 *Physica C* **290** 291
 - [11] Yang Z J and Hull J R 1997 *IEEE Trans. Appl. Supercond.* **7** 318
 - [12] Sanchez A and Navau C 1996 *Physica C* **268** 46
 - [13] Navau C and Sanchez A 1998 *Phys. Rev. B* **58** 963
 - [14] Kordyuk A A 1998 *J. Appl. Phys.* **83** 610
 - [15] Sanchez A and Navau C 2001 *Phys. Rev. B* **64** 214506
 - [16] Navau C and Sanchez A 2001 *Phys. Rev. B* **64** 214507
 - [17] Qin M J, Li G, Liu H K, Dou S X and Brandt E H 2001 *Preprint cond-mat/0111316*
 - [18] Clem J R and Sanchez A 1994 *Phys. Rev. B* **50** 9355
 - [19] Navau C and Sanchez A 2002 *Physica C* in press
 - [20] Navau C and Sanchez A 1997 *IEEE Trans. Appl. Super-*

cond. **7** 920

- [21] Forkl A 1993 *Phys. Scr.* **T49** 148

FIG. 1: Geometry and dimensions of the considered superconductor-permanent magnet system (left). Sketch of a minor loop running between z_1 and z_2 (right).

FIG. 2: Vertical levitation force for a complete major loop and for several minor loops of amplitude $\Delta z=0.005\text{m}$ produced every 0.005m . Other parameters of the calculated case are in the text. In the inset there is a zoom of one of the minor loops. The current penetration profiles in the marked points are shown in Fig. 3.

FIG. 3: Current penetration profiles for a semi plane of constant angle (the z -axis is at left in every figure) at several distances during a minor loop. The distances are the ones marked in Fig. 2. Currents induced during the descend of the minor loop (increase of the applied field) are drawn in dark gray. In light gray there are the reverse currents induced during the ascent of the superconductor.

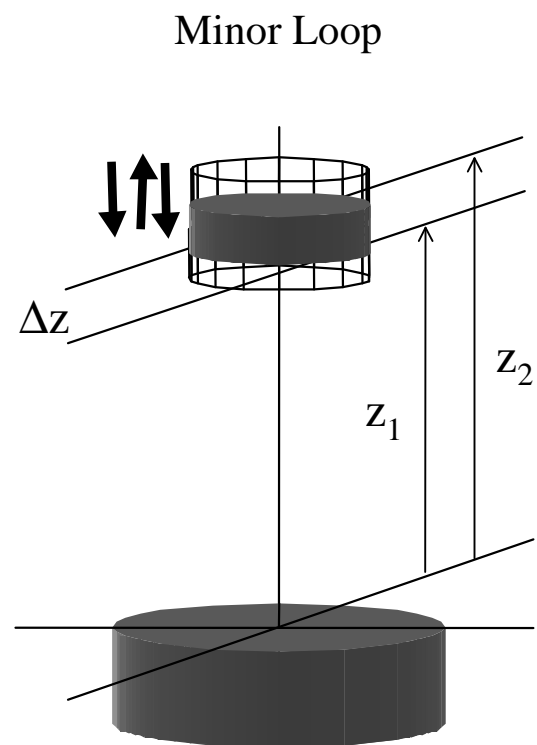
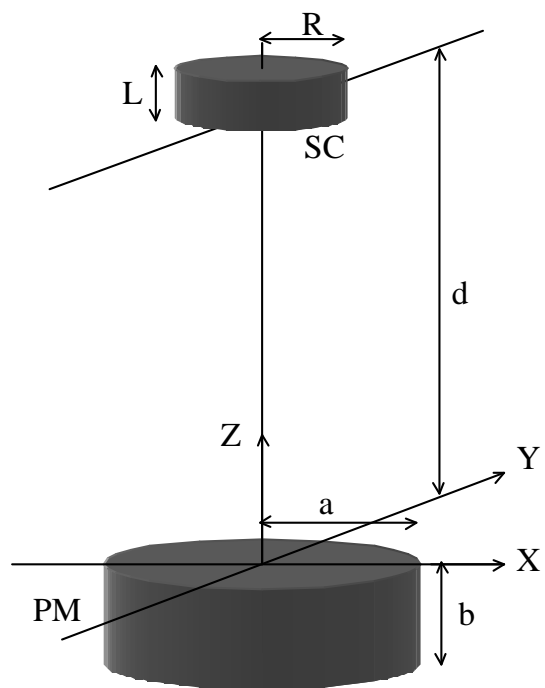
FIG. 4: (a) Vertical stiffness κ_{zz} and (b) hysteretic energy losses E_{zz} as a function of the critical current of the superconductor. The PM is fixed and the aspect ratio of the superconductor is changed by changing the value of L such that $L/R=0.2$ (dotted line), $L/R=1$ (solid line), and $L/R=5$ (dashed line). Other parameters are written in the text.

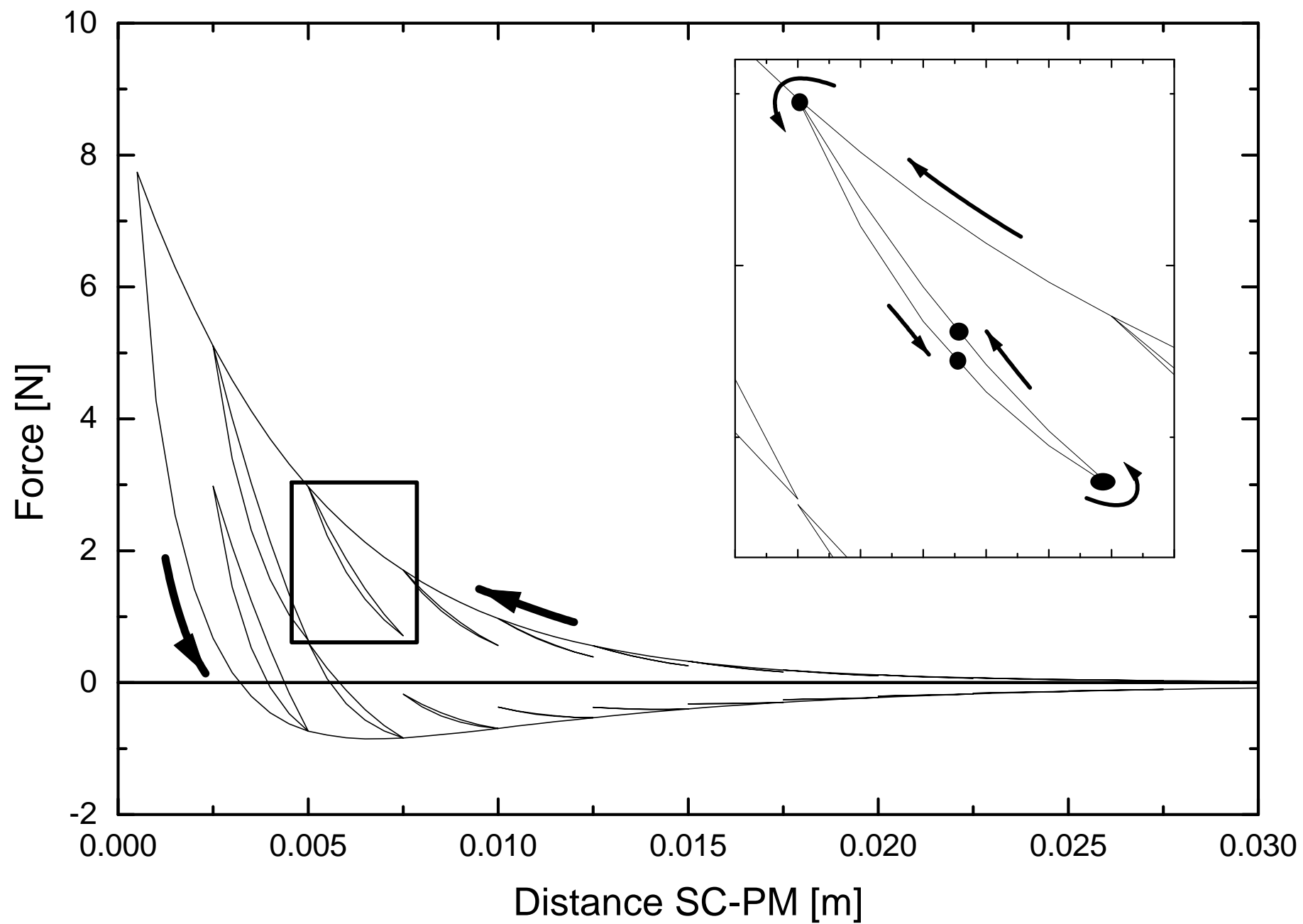
FIG. 5: Force versus distance minor loops started at $z_1=0.005\text{m}$ and of amplitude $\Delta z=0.0025\text{m}$ for the cases (a) $L/R = 0.2$, (b) $L/R = 1$, and (c) $L/R = 5$. The values of J_c have been chosen to be equally spaced in logarithm scale and they range (from lower to higher maximum force —thinner to thicker line) (a) from $J_c = 1.000 \cdot 10^6 \text{A/m}^2$ to $J_c = 5.623 \cdot 10^7 \text{A/m}^2$; (b) and (c) from $J_c = 1.000 \cdot 10^7 \text{A/m}^2$ to $J_c = 5.623 \cdot 10^8 \text{A/m}^2$. For comparison, the loop corresponding to $J_c = 1.000 \cdot 10^7 \text{A/m}^2$ is showed as a dotted line.

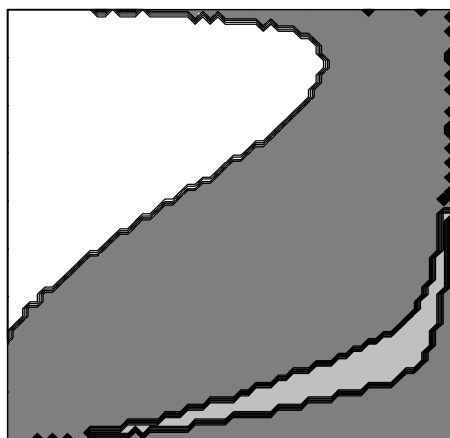
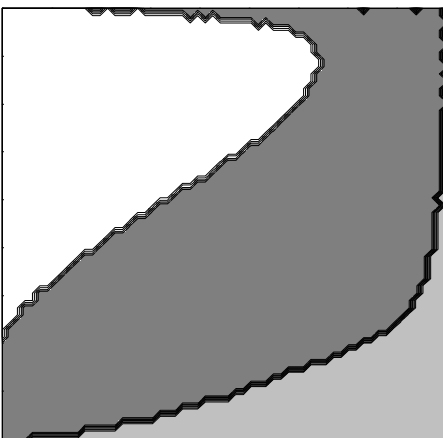
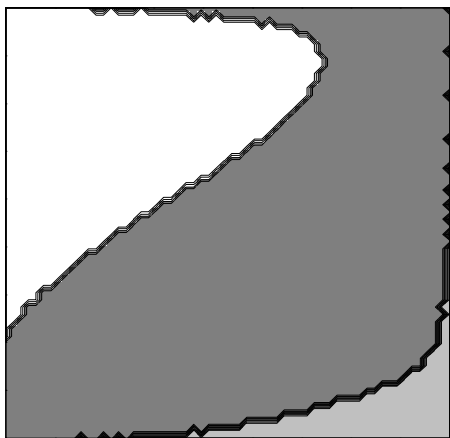
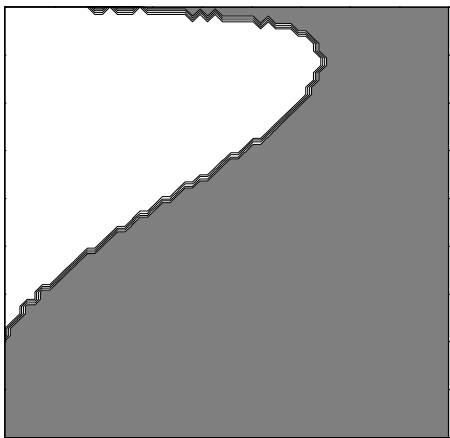
FIG. 6: (a) Vertical stiffness κ_{zz} and (b) hysteretic energy losses E_{zz} as a function of the aspect ratio of the superconductor, for different values of the critical current: $J_c R/H_0=0.1$ (solid line), $J_c R/H_0=1$ (dot-dashed line). Other parameters are written in the text.

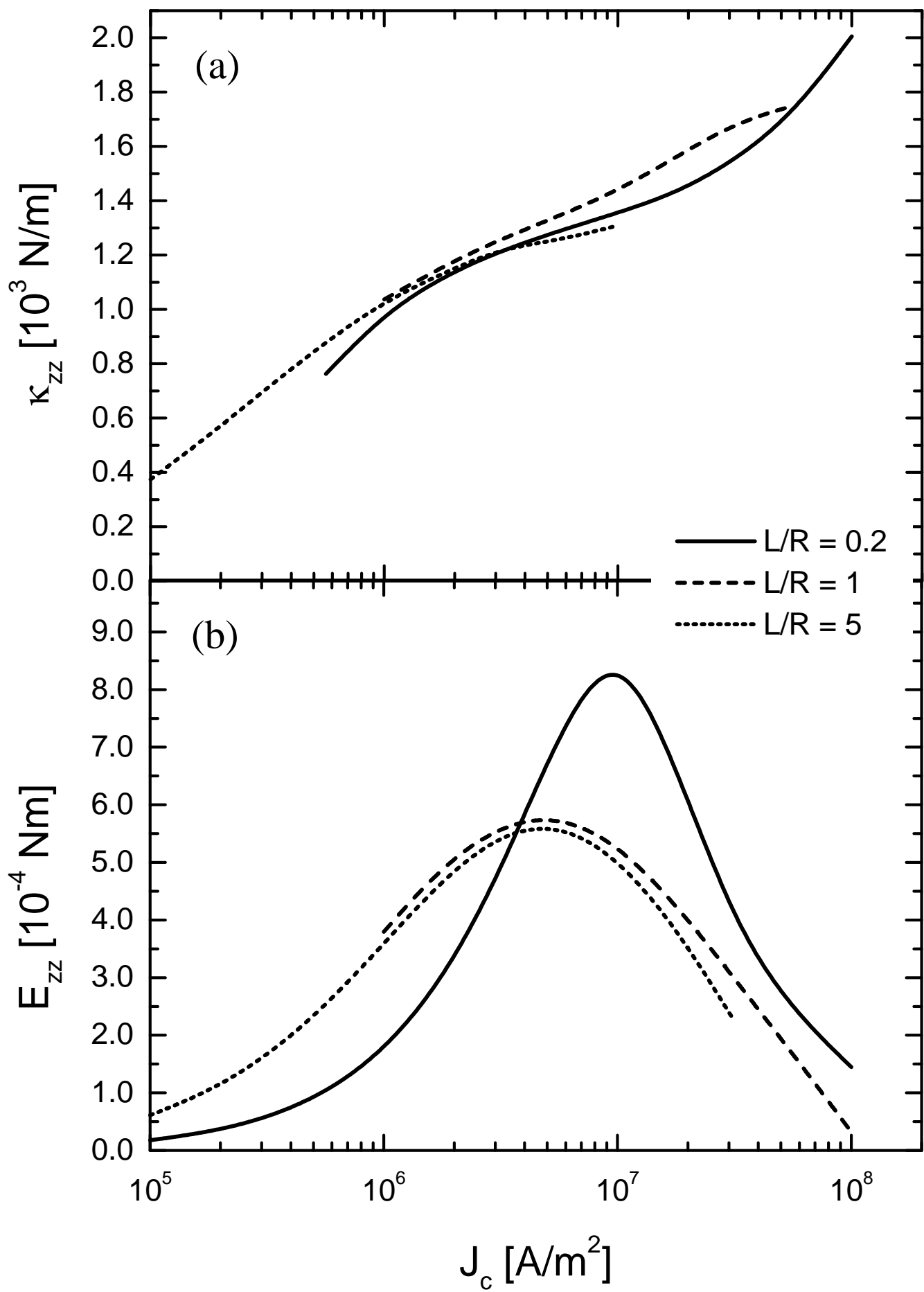
FIG. 7: Force versus distance minor loops started at $z_1=0.005\text{m}$ and of amplitude $\Delta z=0.0025\text{m}$ for the cases (a) $J_c R/H_0=0.1$ and (b) $J_c R/H_0=1$. The value of L/R is (from lower to higher maximum force —thinner to thicker line) $L/R = 0.1, 0.5, 1.0, 1.5$, and 2.0 , respectively.

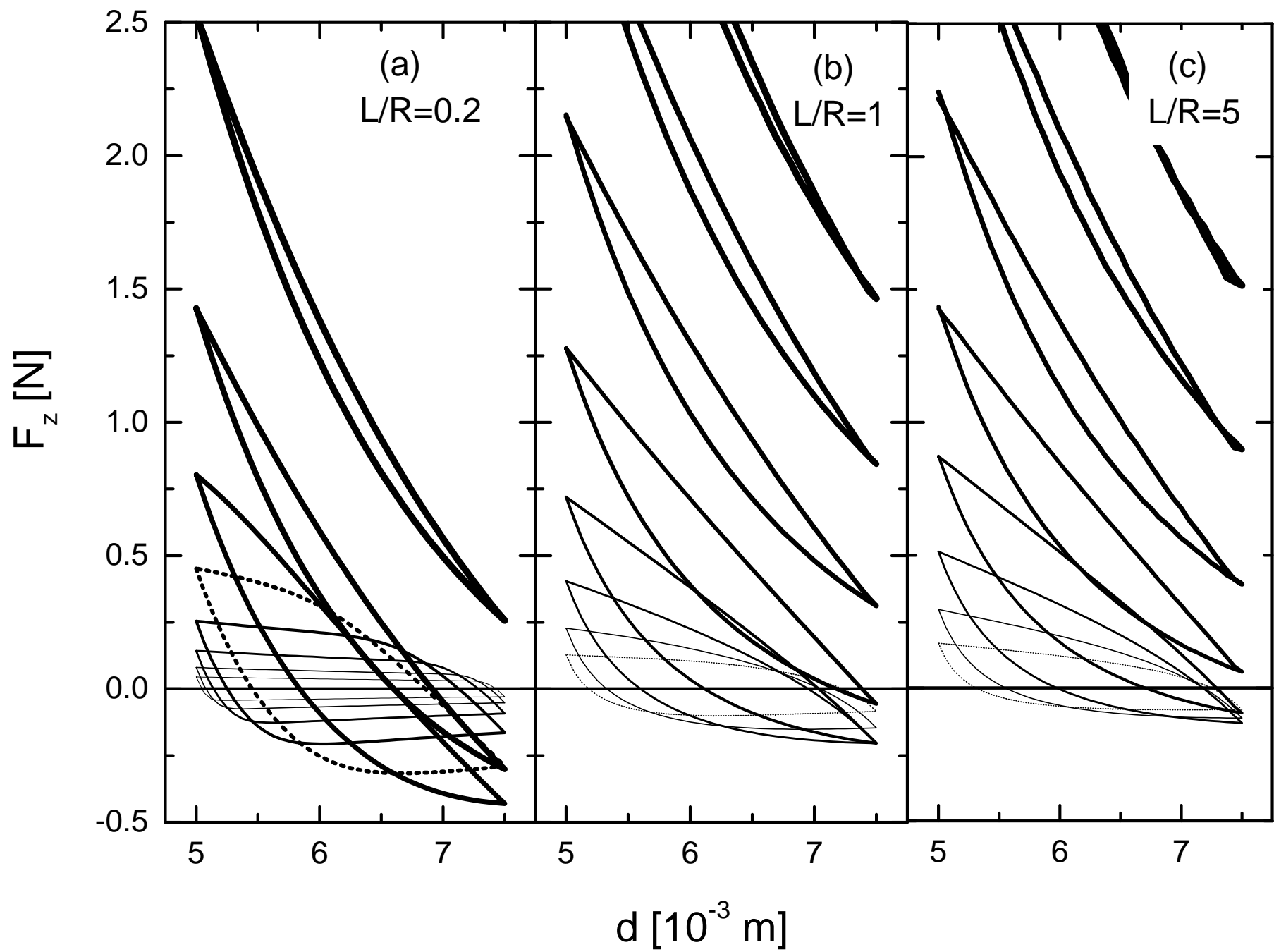
FIG. 8: (a) Vertical stiffness κ_{zz} and (b) hysteretic energy losses E_{zz} as a function of the relative radius of the PM and the superconductor a/R , for different values of the critical current: $J_c R/H_0=0.1$ in dotted line and $J_c R/H_0=1$ in solid line. Other parameters are written in the text.

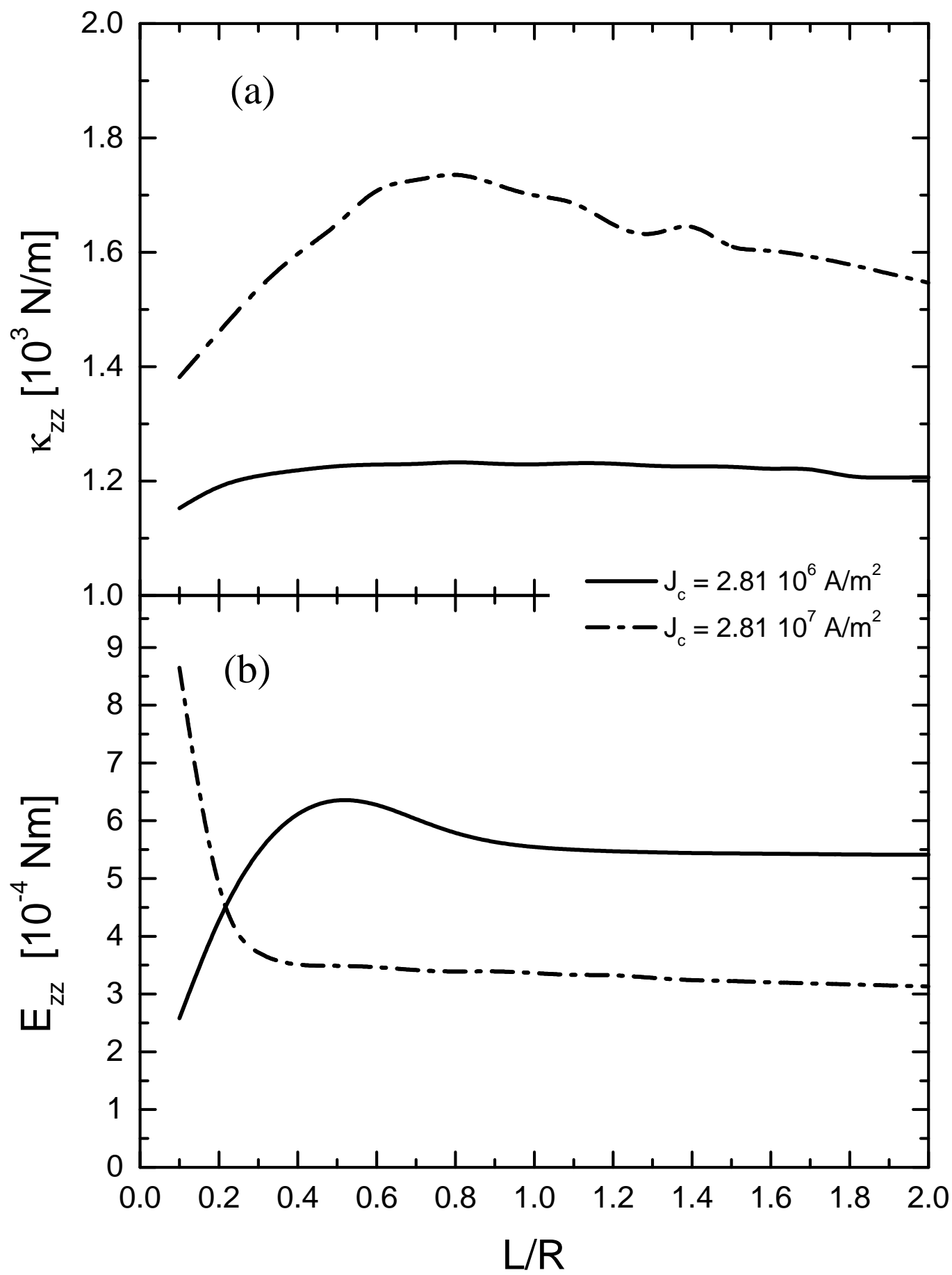


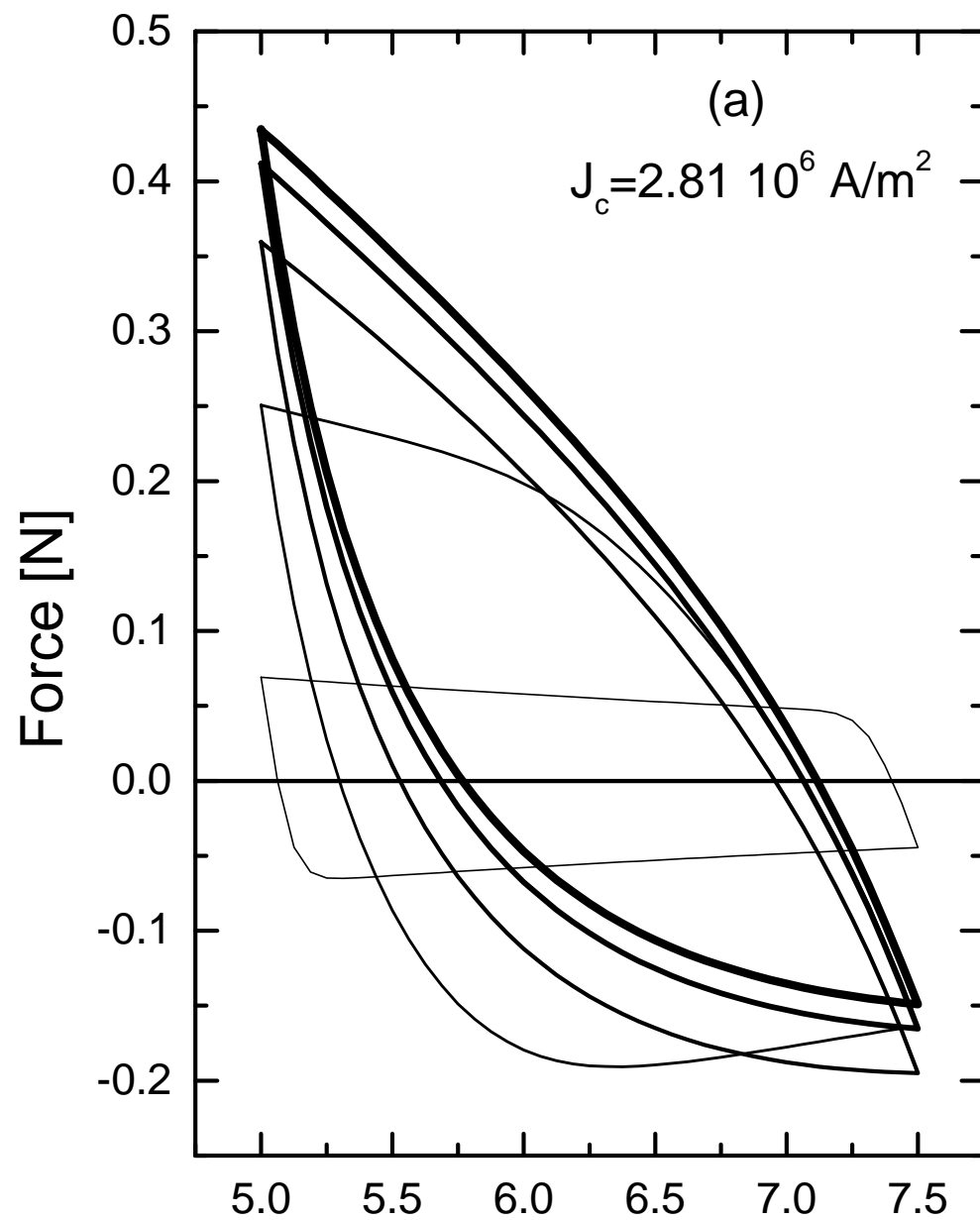












$d [10^{-3} \text{ m}]$

